BULLETIN OF THE POLISH ACADEMY OF SCIENCES
TECHNICAL SCIENCES, Vol. 67, No. 3, 2019
DOI: 10.24425/bpasts.2019.129645

Chaos synchronization of uncertain coronary artery systems through sliding mode

D.W. QIAN[1,3]*, Y.F. XI[1], and S.W. TONG[2]

[1] School of Control and Computer Engineering, North China Electric Power University, Beijing, 102206, P.R. China
[2] College of Robotics, Beijing Union University, Beijing, 100101, P.R. China
[3] State Key Laboratory of Management and Control for Complex Systems, Institute of Automation, Chinese Academy of Sciences, Beijing, 100190, P.R. China

Abstract. The chaotic phenomena of coronary artery systems are hazardous to health and may induce illness development. From the perspective of engineering, the potential harm can be eliminated by synchronizing chaotic coronary artery systems with a normal one. This paper investigates the chaos synchronization problem in light of the methodology of sliding mode control (SMC). Firstly, the nonlinear dynamics of coronary artery systems are presented. Since the coronary artery systems suffer from uncertainties, the technique of derivative-integral terminal SMC is employed to achieve the chaos synchronization task. The stability of such a control system is proven in the sense of Lyapunov. To verify the feasibility and effectiveness of the proposed method, some simulation results are illustrated in comparison with a benchmark.

Key words: chaos synchronization, coronary artery systems, sliding mode control, nonlinear dynamics.

1. Introduction

Coronary artery disease has dominated mortality for most of the past century worldwide [1]. Its treatments, both pharmaceutical and surgical, have become leading sectors of the healthcare economy. In 2015, coronary artery disease affected 110 million people and resulted in 8.9 million deaths [2]. In order to explore new treatment options, both the medical and engineering communities try to provide some insight into coronary artery disease.

From the aspect of medicine, coronary arteries act as the blood vessels that supply oxygen-rich blood to the heart muscle. In case plaque builds up inside the coronary arteries, the buildup of plaque gradually obstructs the coronary arteries. Such obstruction may lead to vascular spasm. The vasospasms constitute the basic cause of a variety of coronary artery disease. Some drugs have been developed via the mechanism [3].

In the field of engineering, a coronary artery system consists of the bio-mathematical model of blood vessels, where the vasospasms are the chaotic states of the blood vessels [4]. Since chaotic systems are sensitive to perturbations, the chaotic phenomenon may result in fatal chaos in the coronary arteries [5]. The chaotic phenomenon must be suppressed to avoid serious health problems and illness development. In order for treatment to be effective, the chaotic suppression has to achieve the state synchronization of the blood vessels with the pathological changes and the normal blood vessels.

The state synchronization problem of a chaotic system was proposed by Pecora and Carroll [6]. Since then, the solution of this problem has become emerging because of lots of potential applications. Many synchronization approaches have been developed for various systems. The approaches can be roughly cataloged into two classes, that is, linear or partial linearisation methods [7, 8] and nonlinear approaches [9, 10]. Especially, linear or partial linearisation methods are just appropriate for stable linear systems that are characterised by a few distinct peaks in their power spectrum.

Concerning the coronary artery system, this complex biosystem is inherently nonlinear and requires nonlinear methods to achieve its state synchronization. The research topic has been paid more and more attention and some reports can be seen. Some synchronization methods have been reported. Gong, Li and Sun [12] developed a backstepping-based controller to synchronize the spastic vessel with a normal vessel. Li [5] designed a nonlinear tracking controller and the controller could robustly and adaptively drive a chaotic coronary artery system into the normal orbit. Wu et al [11] considered the drug absorption time and presented the time-delay state feedback control synthesis.

As a nonlinear design tool, the methodology of sliding mode control (SMC) is advocated for its invariance [13–15]. The invariance means that a SMC system on the sliding-mode stage is completely insensitive to parametric uncertainties and external disturbances under certain matching conditions [16–18]. The characteristic makes the SMC exhibit better performances than other robust control methods. In practice, Lin, Yang and Yau [19] have investigated that the SMC-based method can be carried out for the chaotic suppression problem of coronary artery systems. Zhao and his colleagues also have applied the higher-order sliding mode control [24] and the terminal sliding mode control [20] for the same chaotic suppression problem.

*e-mail: dianwei.qian@ncepu.edu.cn

Manuscript submitted 2018-01-28, revised 2018-07-03 and 2018-09-04, initially accepted for publication 2018-10-01, published in June 2019.

The terminal sliding mode control (T-SMC) method is characterized by its terminal sliding surface. Usually, the method has faster convergence speed and higher steady-state accuracy than other SMC methods [21, 22]. As an extension, the integral T-SMC method introduces sign and fractional integral terminal sliding mode concepts, it allows a system to start on the integral terminal sliding surface, and it is able to track relative-degree-one systems with uncertainties and disturbances [23]. Furthermore, the derivative-integral T-SMC method, a further progress of the extension, is derived to track high-order systems because it can guarantee the exact estimation of finite error convergence time [25].

Motivated by the merits of the progress, this paper investigates the derivative-integral T-SMC method for the chaos synchronization problem in a coronary artery system. The purpose of the paper is to reduce the occurrence of coronary artery disease by rejecting the abnormal chaotic behaviors of the coronary artery system. Even when they have different initial conditions, the abnormal chaotic behaviors can still be synchronized with the normally unstable periodic orbit. For this purpose, the derivative-integral T-SMC method is adopted to achieve the behavior synchronization.

Moreover, the coronary artery system suffers from external disturbances such as the perturbations of blood pressure, blood viscosity and body temperature in reality. The external disturbances challenge the chaos synchronization problem very much because they are unknown and unpredictable [26–28]. In the sense of Lyapunov, the stability of the synchronization control system with uncertainties is analyzed. Compared with some published results, the feasibility and effectiveness of the solution is illustrated via some numerical results.

The remainder of this paper is organized as follows. Section 2 introduces the bio-mathematical model of the coronary artery system. Section 3 formulates the control problem. The synchronization control via the derivative-integral T-SMC-based controller is derived in Section 4 for the coronary artery system. To show the synchronization performance, some numerical simulations are carried out in Section 5. Finally, conclusions are drawn in Section 6.

2. Bio-mathematical model

Inherently, coronary arteries are a kind of muscular blood vessels. Concerning a coronary artery system, the lumped-parameter model that describes its dynamics [19] has the form of

$$\begin{aligned} \dot{x}_1 &= -bx_1 - cx_2\,, \\ \dot{x}_2 &= -\lambda(1+b)x_1 - \lambda(1+c)x_2 + \lambda x_1^3 + E\cos\omega t\,, \end{aligned} \tag{1}$$

where x_1 is the inradius change of the vessel, x_2 means the pressure change in the vessel, t indicates the time variable, b, c and λ denote lumped parameters of the coronary artery system and $E\cos\omega t$ represents a periodical disturbance term.

As one factor that results in myocardial infarction, coronary artery spasm is caused by partial or complete occlusion of coronary arteries [1]. (1) reveals the medical phenomenon from the perspective of mathematics. In (1), the initial condition $[x_1(0)\ x_2(0)]^T = [0.2\ 0.2]^T$ is taken into consideration, where the parameters E and ω are determined by 0.3 and 1, respectively.

Fig. 1 shows the bifurcation diagram of the coronary artery system (1) with respect to the change of λ, where another parameters are set by $b = 0.15$ and $c = -1.7$. Fig. 2 reveals the bifurcation diagram of the coronary artery system (1) with respect to the change of b, where another parameters are set by $\lambda = -0.65$ and $c = -1.7$. Fig. 3 shows the bifurcation diagram

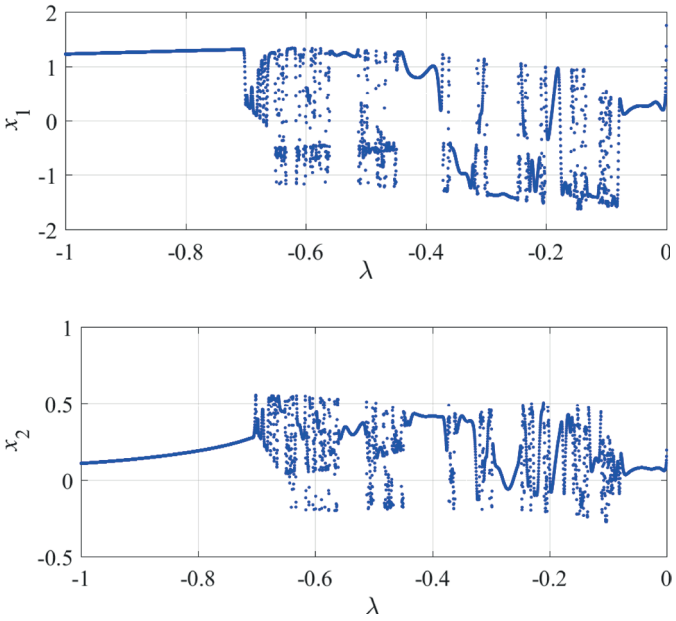

Fig. 1. Bifurcation diagrams with respect to the change of λ from -1 to 0.

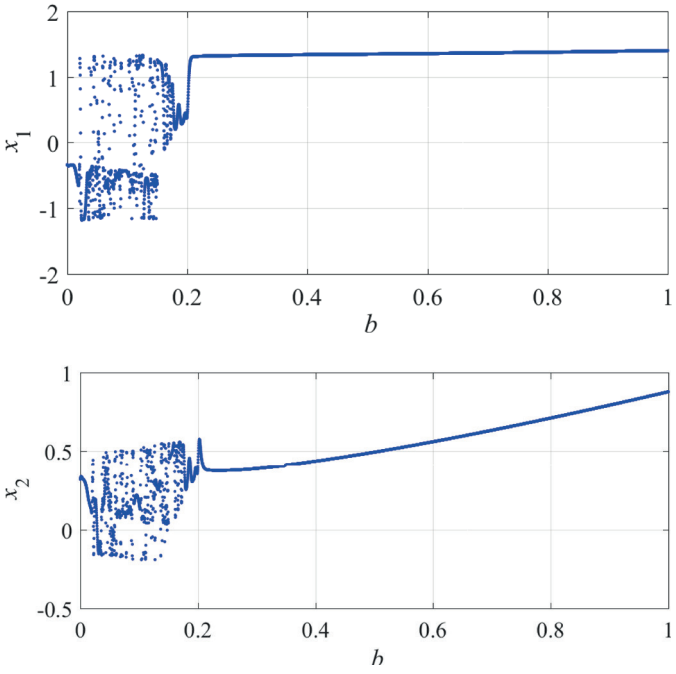

Fig. 2. Bifurcation diagrams with respect to the change of b from 0 to 1.

of the coronary artery system (1) with respect to the change of c, where another parameters are set by $\lambda = -0.65$ and $b = 0.15$. All the bifurcation diagrams share the aforementioned initial condition. The time series are set by 0, 2π, 4π, 6π, 10π and 12π, where the system period is 2π.

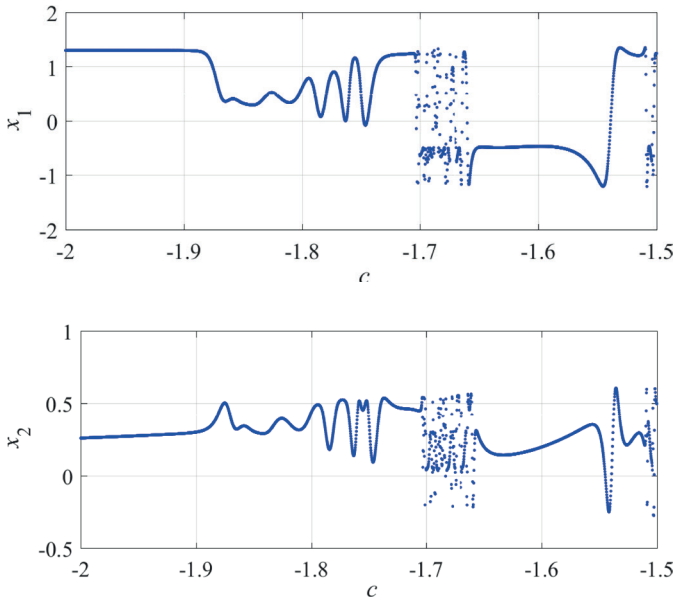

Fig. 3. Bifurcation diagrams with respect to the change of c from -2 to -1.5.

The bifurcation diagrams in Figs 1–3 illustrate that the coronary artery system under some parameters is disordered and will lead to chaos. As far as the coronary artery system is concerned, the following lumped parameters are considered, that is, $\lambda = -0.65$, $b = 0.15$, $c = -1.7$, $E = 0.3$ and $\omega = 1$. With the group of lumped parameters, Fig. 4 illustrates the coronary artery system has very complex dynamics in the phase plane.

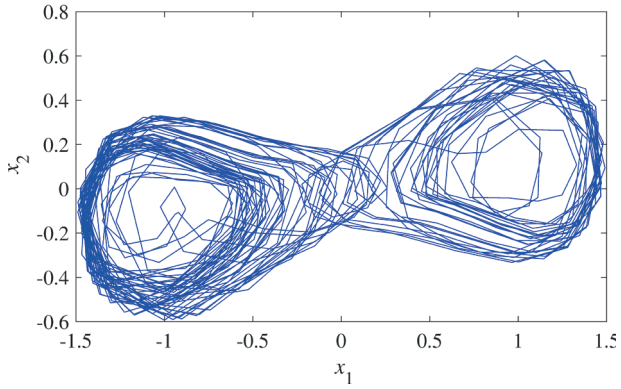

Fig. 4. Phase plane of the coronary artery system.

From Figs 1–4, the coronary artery system is apparently disordered with respect to the changes of these lumped parameters. The coronary artery system may descend into chaos under some initial conditions with respect to the change of the lumped parameters. The chaotic behaviors in clinic medicine indicate that the vascular spasm of the coronary artery system may exhibit a series of coronary artery disease, including but not limited to angina, myocardial infarction, and sudden cardiac death. The chaos may extremely hazard health and must be suppressed immediately. Since the chaos synchronization problem of such a coronary artery system is challenging and interesting, this paper explores the problem from the aspect of control design via derivative-integral terminal sliding mode.

3. Control problem formulation

From the bio-mathematical model (1), the coronary artery system with uncertainties (2) can be drawn

$$\begin{aligned} \dot{x}_1 &= -bx_1 - cx_2 + d_1\,, \\ \dot{x}_2 &= -\lambda(1+b)x_1 - \lambda(1+c)x_2 + \lambda x_1^3 \\ &\quad + E\cos\omega t + u(t) + d_2\,. \end{aligned} \tag{2}$$

Here $\mathbf{x} = [x_1,\ x_2]^T$ is defined as the state vector and $u(t)$ generated by the designed controller is the control input. The vector $\mathbf{d} = [d_1,\ d_2]$ describes the uncertainties, meaning unmodelled dynamics, external disturbances and structural variations.

Assumption 1. $\mathbf{d}$ is bounded, that is, $||\mathbf{d}||_\infty \le d^*$, where d^* is a known positive constant.

Assumption 2. $\mathbf{d}$ is slowly time varying, that is, $\dot{\mathbf{d}} \simeq \mathbf{0}_{2\times 1}$, where $\mathbf{0}_{2\times 1} = [0,\ 0]^T$.

From (2), the nominal system of the coronary artery system with no control input can be written as

$$\begin{aligned} \dot{\bar{x}}_1 &= -b\bar{x}_1 - c\bar{x}_2\,, \\ \dot{\bar{x}}_2 &= -\lambda(1+b)\bar{x}_1 - \lambda(1+c)\bar{x}_2 + \lambda\bar{x}_1^3 + E\cos\omega t\,. \end{aligned} \tag{3}$$

Concerning the bio-mathematical model (1), (3) can display different dynamics because it is highly sensitive to its parameters. This fact means that even small differences of the parameters yield widely diverging outcomes of the chaotic behaviors. Consequently, the purpose of chaos synchronization in the coronary artery system is to synchronize the uncertain coronary artery system (2) with the nominal system (3) via derivative-integral terminal sliding mode, that is,

$$\lim_{t\to\infty} \mathbf{e} = \mathbf{0}_{2\times 1}\,. \tag{4}$$

Here $\mathbf{e} = [e_1,\ e_2]$, $e_1 = x_1 - \bar{x}_1$ and $e_2 = x_2 - \bar{x}_2$

Considering (2), (3) and (4), the error system can be described by

$$\begin{aligned} \dot{e}_1 &= -be_1 - ce_2 + d_1\,, \\ \dot{e}_2 &= -\lambda(1+b)e_1 - \lambda(1+c)e_2 + \lambda e_1^3 \\ &\quad + 3\lambda x_1\bar{x}_1 e_1 + u + d_2\,. \end{aligned} \tag{5}$$

Further, define $\tilde{x}_1 = e_1$ and $\tilde{x}_2 = \dot{e}_1$ and differentiate $\tilde{x}_1$ and $\tilde{x}_2$ with respect to the time variable t. Then, substituting (5) into $\dot{\tilde{x}}_2$

has the form of

$$\begin{aligned}\dot{\tilde{x}}_1 &= \tilde{x}_2\,,\\ \dot{\tilde{x}}_2 &= \lambda\,(c-b)\,\tilde{x}_1 - (b+\lambda+c\lambda)\,\tilde{x}_2 - \lambda c\tilde{x}_1^3 - 3c\lambda x_1\bar{x}_1\tilde{x}_1\\ &\quad - cu - cd_2 + \dot{d}_1 + \lambda\,(1+c)\,d_1\,.\end{aligned} \tag{6}$$

According to Assumption 2, $\dot{d}_1 \simeq 0$ in (6). Then, (6) can be written by (7) in the form of state space.

$$\begin{aligned}\dot{\tilde{\mathbf{x}}} &= F\,(\tilde{\mathbf{x}},d) + Bu,\\ y &= H\,(\tilde{\mathbf{x}})\,.\end{aligned} \tag{7}$$

Here $\tilde{\mathbf{x}} = [\tilde{x}_1,\ \tilde{x}_2]^T$, $d = -cd_2 + \lambda\,(1+c)\,d_1$, $H\,(\tilde{\mathbf{x}}) = \tilde{x}_1$, $B = [0,\ -c]^T$, $F\,(\tilde{\mathbf{x}},d) = [\tilde{x}_2,\ f(\tilde{\mathbf{x}}) + d]^T$ and $f(\tilde{\mathbf{x}}) = \lambda\,(c-b)\,\tilde{x}_1 - (b+\lambda+c\lambda)\,\tilde{x}_2 - \lambda c\tilde{x}_1^3 - 3c\lambda x_1\bar{x}_1\tilde{x}_1$.

Assumption 3. The functions $F(\tilde{\mathbf{x}},d)$ and $H(\tilde{\mathbf{x}})$ are sufficiently smooth so all Lie derivative calculations are well-defined.

Proven by Chiu [25], the derivative-integral T-SMC design can be available for high relative-degree systems that have higher relative degree than 1. According to Assumption 3, the relative degree of (7) can be calculated as (8), (9) and (10) in order to develop the derivative-integral T-SMC design for (7).

$$L_B H\,(\tilde{\mathbf{x}},d) = \frac{\partial H\,(\tilde{\mathbf{x}},d)}{\partial \tilde{\mathbf{x}}} B = \begin{bmatrix}1 & 0\end{bmatrix} \times \begin{bmatrix}0\\ -c\end{bmatrix} = 0, \tag{8}$$

$$L_F H\,(\tilde{\mathbf{x}},d) = \frac{\partial H\,(\tilde{\mathbf{x}},d)}{\partial \tilde{\mathbf{x}}} F = \begin{bmatrix}1 & 0\end{bmatrix} \times \begin{bmatrix}\tilde{x}_2\\ f(\tilde{\mathbf{x}}) + d\end{bmatrix} = \tilde{x}_2\,, \tag{9}$$

$$\begin{aligned}L_B L_F H\,(\tilde{\mathbf{x}},d) &= L_B\,(L_F H\,(\tilde{\mathbf{x}},d)) = \frac{\partial\,(L_F H\,(\tilde{\mathbf{x}},d))}{\partial \tilde{\mathbf{x}}} B\\ &= \begin{bmatrix}0 & 1\end{bmatrix} \times \begin{bmatrix}0\\ -c\end{bmatrix} = -c \neq 0.\end{aligned} \tag{10}$$

From (8), (9) and (10), the relative degree of (7) can be determined as 2 so that it is possible to develop a derivative-integral terminal sliding mode controller for the chaos synchronization [25]. Furthermore, the input-output dynamics can be expressed as

$$\ddot{y} = L_F^2 H\,(\tilde{\mathbf{x}},d) + L_B L_F H\,(\tilde{\mathbf{x}},d)\,u. \tag{11}$$

Here $L_F^2 H\,(\tilde{\mathbf{x}},d) = \dfrac{\partial\,(L_F H\,(\tilde{\mathbf{x}},d))}{\partial \tilde{\mathbf{x}}} F = f\,(\tilde{\mathbf{x}}) + d$. Then, (11) can be written by

$$\ddot{y} = f\,(\tilde{\mathbf{x}}) + d - cu. \tag{12}$$

4. Derivative-integral T-SMC design

This paper investigates the derivative-integral T-SMC method for the chaos synchronization problem. The so-called derivative-integral terminal sliding mode means that the derivative and integral terms exist in a sliding surface. Motivated by this purpose, the following sliding surface s is taken into consideration.

$$s = e_{D1} + \alpha e_{I1}\,. \tag{13}$$

Here $\alpha > 0$ is a design parameter, $e_{D1} = \dot{e}_{D0}^{p_{11}/q_{11}} + \beta e_{D0}$, $e_{D0} = e_1$, $\dot{e}_{I1} = e_{D1}^{q_{21}/p_{21}}(t)$ and $e_{I1}(0) = -\dfrac{e_{D1}(0)}{\alpha}$, where $\beta > 0$ is pre-defined and $p_{11} > q_{11} > 0$ chosen by designers are odd integers, as well as $p_{21} > q_{21} > 0$.

Theorem 1. If the sliding surface is defined as (13), then $[\tilde{x}_1,\ \tilde{x}_2]^T$ in (6) will reach $\mathbf{0}_{2\times 1}$ in the finite convergence time τ_{DI}, where τ_{DI} is formulated by

$$\tau_{DI} = \frac{|e_{D_1}(0)|^{1-\frac{q_{21}}{p_{21}}}}{\alpha\left(1-\dfrac{q_{21}}{p_{21}}\right)} + \frac{|e_{D_0}(t_{11})|^{1-\frac{q_{11}}{p_{11}}}}{\beta\left(1-\dfrac{q_{11}}{p_{11}}\right)}. \tag{14}$$

Here t_{11} is the reaching time of the sliding mode $e_{D1} = 0$.

Proof. From (13), the sliding mode starts at $t = 0$. From then on, $e_{D1} = -\alpha e_{I1}$ can always hold true via control design. Subsequently, substituting $e_{D1} = -\alpha e_{I1}$ into $\dot{e}_{I1} = e_{D1}^{q_{21}/p_{21}}(t)$ yields

$$\dot{e}_{I1} = -\alpha^{\frac{q_{21}}{p_{21}}} e_{I1}^{\frac{q_{21}}{p_{21}}}, \tag{15}$$

where $e_{I1}(0) = -e_{D1}(0)/\alpha$.

Solving (15), the convergent time of e_{I1} can be gotten as

$$t_{11} = \frac{|e_{D_1}(0)|^{1-\frac{q_{21}}{p_{21}}}}{\alpha\left(1-\dfrac{q_{21}}{p_{21}}\right)}. \tag{16}$$

On the sliding surface $s = 0$, $e_{D1} = -\alpha e_{I1}$ indicates that the sliding mode of e_{D1} takes place at the same time t_{11} to zero. When $e_{D1} = 0$, e_{D0} will successively converge to zero. At $t = t_{11}$, e_{D0} can be formulated by

$$\dot{e}_{D_0}(t_{11}) = -\beta^{\frac{q_{11}}{p_{11}}} e_{D_0}^{\frac{q_{11}}{p_{11}}}(t_{11}). \tag{17}$$

From (17), the time spent from $e_{D0}(t_{11})$ to $e_{D0} = 0$ can be calculated as

$$t_{01} = \frac{|e_{D_0}(t_{11})|^{1-\frac{q_{11}}{p_{11}}}}{\beta\left(1-\dfrac{q_{11}}{p_{11}}\right)}. \tag{18}$$

According to (16) and (18), the time spent from $s(0) = 0$ to $e_1 = 0$ is their summation because the integral and derivative terms in (13) are independent. Consequently, the finite convergence time can have the form of (14), that is, $\tau_{DI} = t_{11} + t_{01}$. □

Remark 1. At $t = 0$, $s = e_{D1}(0) + \alpha e_{I1}(0)$. Considering the definition $e_{I1}(0) = -\dfrac{e_{D1}(0)}{\alpha}$, we have $s = 0$ at $t = 0$. This fact indicates that the sliding mode of the control design takes place at the time $t = 0$.

Theorem 2. Consider the bio-mathematical model of the coronary artery system (2); take Assumptions 1, 2 and 3 into account; define the error system (5) and have the input-output dynamics (12); formulate the derivative-integral terminal sliding surface (13). If the derivative-integral T-SMC law is formulated by (19), the closed-loop chaos synchronization system is then asymptotically stable in the presence of uncertainties.

$$u = -\frac{1}{c}\left[-k_e|\psi|\left(\frac{q_{11}}{p_{11}}\right)A^{-1}\frac{s}{|s|} - f(\tilde{\mathbf{x}}) - [\kappa\,\mathrm{sgn}(s)+\eta s] - d_0^*\right], \tag{19}$$

where $A = \begin{cases} \dot{e}_{D01}^{\left(\frac{p_{11}}{q_{11}}-1\right)}, & \text{for } \left|\dot{e}_{D01}^{\left(\frac{p_{11}}{q_{11}}-1\right)}\right| \geq \varepsilon \\ \varepsilon, & \text{otherwise} \end{cases}$, $\kappa > d_0^* - d > 0$, $d_0^* = [|c| + |\lambda(1+c)|]d^*$, $k_e > \dfrac{1}{1-\phi}$, $0 < \phi < 1$ and $\eta > 0$.

Proof. In order to obtain the derivative-integral T-SMC law, a Lyapunov candidate is selected as $V_0 = \frac{1}{2}s^2$. Differentiate V_0 with respect to the time variable t. $\dot{V}_0 = s\dot{s}$ can be obtained. Further, the derivative of s can be formulated by

$$\dot{s} = \frac{p_{11}}{q_{11}}\dot{e}_{D0}^{\left(\frac{p_{11}}{q_{11}}-1\right)}\ddot{e}_{D0} + \beta\dot{e}_{D0} + \alpha\left(\dot{e}_{D0}^{\frac{p_{11}}{q_{11}}} + \beta e_{D0}\right)^{\frac{q_{21}}{p_{21}}}. \tag{20}$$

Substituting (12) into (20) yields

$$\dot{s} = \frac{p_{11}}{q_{11}}\dot{e}_{D0}^{\left(\frac{p_{11}}{q_{11}}-1\right)}[f(\tilde{\mathbf{x}}) + d - cu] + \psi, \tag{21}$$

where $\psi = \beta\dot{e}_{D0} + \alpha\left(\dot{e}_{D0}^{\frac{p_{11}}{q_{11}}} + \beta e_{D0}\right)^{\frac{q_{21}}{p_{21}}}$.

Replacing $\dot{s}$ in $\dot{V}_0$ by (21) gives

$$\dot{V}_0 = s\frac{p_{11}}{q_{11}}\dot{e}_{D0}^{\left(\frac{p_{11}}{q_{11}}-1\right)}[f(\tilde{\mathbf{x}}) + d - cu] + s\psi. \tag{22}$$

Consider the derivative-integral T-SMC law (19). Then, (22) can be written by

$$\dot{V}_0 = s\psi - s\dot{e}_{D0}^{\left(\frac{p_{11}}{q_{11}}-1\right)}k_e|\psi|A^{-1}\frac{s}{|s|} + s\frac{p_{11}}{q_{11}}\dot{e}_{D0}^{\left(\frac{p_{11}}{q_{11}}-1\right)}[d - d_0^* - (\kappa\,\mathrm{sgn}(s)+\eta s)]. \tag{23}$$

Owing to $p_{11} > 0$, $q_{11} > 0$ and $p_{11} > q_{11}$, $\dfrac{p_{11}}{q_{11}} > 1$ exists such that $\dot{e}_{D01}^{\left(\frac{p_{11}}{q_{11}}-1\right)} > 0$ holds true in (19) for all $\dot{e}_{D01}^{\left(\frac{p_{11}}{q_{11}}-1\right)} \neq 0$. Consequently, the first and second terms in (23) can have the form of

$$\begin{aligned} & s\psi - s\dot{e}_{D0}^{\left(\frac{p_{11}}{q_{11}}-1\right)}k_e|\psi|A^{-1}\frac{s}{|s|} \\ &= s\psi - k_e|\psi|s + k_e|\psi|AA^{-1}s - s\dot{e}_{D0}^{\left(\frac{p_{11}}{q_{11}}-1\right)}k_e|\psi|A^{-1}\frac{s}{|s|} \\ &\leq |\psi s| - k_e|\psi s| + k_e\left|\psi\left(A - \dot{e}_{D0}^{\left(\frac{p_{11}}{q_{11}}-1\right)}\right)A^{-1}s\right|. \end{aligned} \tag{24}$$

Concerning the expression of A, a parameter $\phi > 0$ exists such that

$$\left|\left(A - \dot{e}_{D01}^{\left(\frac{p_{11}}{q_{11}}-1\right)}\right)A^{-1}\right| \leq \phi < 1. \tag{25}$$

Consequently, (24) can be written by

$$s\psi - s\dot{e}_{D0}^{\left(\frac{p_{11}}{q_{11}}-1\right)}k_e|\psi|A^{-1}\frac{s}{|s|} \leq |\psi s| - k_e(1-\phi)|\psi s|. \tag{26}$$

In order to have $s\psi - s\dot{e}_{D0}^{\left(\frac{p_{11}}{q_{11}}-1\right)}k_e|\psi|A^{-1}\frac{s}{|s|} < 0$, $k_e > \dfrac{1}{1-\phi}$ is picked up.

Further, the third term in (23) can be written by

$$\begin{aligned} & s\frac{p_{11}}{q_{11}}\dot{e}_{D0}^{\left(\frac{p_{11}}{q_{11}}-1\right)}[d - d_0^* - (\kappa\,\mathrm{sgn}(s)+\eta s)] \\ &= \frac{p_{11}}{q_{11}}\dot{e}_{D0}^{\left(\frac{p_{11}}{q_{11}}-1\right)}\left[(d-d_0^*)s - \kappa|s| - \eta s^2\right] \\ &\leq \frac{p_{11}}{q_{11}}\dot{e}_{D0}^{\left(\frac{p_{11}}{q_{11}}-1\right)}\left\{[(d_0^* - d) - \kappa]|s| - \eta s^2\right\}. \end{aligned} \tag{27}$$

In order to have $s\dfrac{p_{11}}{q_{11}}\dot{e}_{D0}^{\left(\frac{p_{11}}{q_{11}}-1\right)}[d - d_0^* - (\kappa\,\mathrm{sgn}(s)+\eta s)] < 0$, $\kappa > d_0^* - d > 0$ and $\eta > 0$ are selected.

From (26) and (27), $\dot{V}_0 < 0$ holds true by the derivative-integral T-SMC design, that is, the control design can synchronize the uncertain coronary artery system. □

Remark 2. From the control design and proof, the uncertainties do not necessarily satisfy the matched condition of the sliding mode control [13]. In fact, they can be either matched or mismatched. Even, they could be mixed uncertainties that contain both matched and mismatched uncertainties.

5. Simulation results

This section presents some numerical simulation results that illustrate the feasibility, validity and robustness of the presented method in comparison with a benchmark. Consider a coronary artery system. Its lumped parameters are fixed to $\lambda = -0.65$, $b = 0.15$, $c = -1.7$, $E = 0.3$ and $\omega = 1$ in (2) and (3). These parameters are kept unchanged from the model presented by [24], as well as the initial states $[\bar{x}_1(0),\ \bar{x}_2(0)]^T = [0.2,\ 0.2]^T$.

Further, the uncertain system (2) contains two disturbance sources, that is, d_1 and d_2. From the viewpoint of sliding mode control, the two disturbances have different characteristics that d_2 is matched and d_1 is mismatched. Further, d_1 and d_2 are merged into d in (6). From the expression of d, both u and d_2 share the same coefficient $-c$. This fact indicates that d_2 is matched. Meanwhile, d_1 can hardly be matched because its coefficient $\lambda(1+c)$ is almost impossible to $-c$.

Pointed out by Utkin [13], the matched uncertainties enter the coronary artery system through the control channel u, so that the control system is insensitive to the uncertainties when the sliding mode is reached. Concerning the presented derivative-integral T-SMC design, its sliding mode takes place at $t = 0$, that is, such a control design is inherently robust regardless of the matched term d_2 in (2) and (6).

In order to demonstrate the robustness of the presented control design, the two kinds of uncertainties will be taken into consideration, respectively. Both d_1 and d_2 are injected to the coronary artery system, separately. Irrespective of the kind of uncertainties, the following parameters of the derivative-integral terminal sliding mode controller are kept unchanged, that is, $\alpha = \beta = 2$, $p_{11} = p_{21} = 9$, $q_{21} = q_{11} = 7$, $\varepsilon = 6$, $\phi = 0.9$, $k_e = 20$ and $\eta = 0.1$.

5.1. Matched uncertainties. In order to illustrate the effects of matched uncertainties, d_1 is set to $2\sin(t)$ and d_2 is set to be 0. Under the condition, the other controller parameters are determined by $d^* = 3.5$, $d_0^* = 7.54$ and $\kappa = 8.0$. Figure 5 displays the presented approach can effectively suppress the chaotic phenomenon under the effects of matched uncertainties. In contrast, the control performance via the method in [24] is not as well as expected although this method can achieve the chaotic suppression. Proven by Theorem 2, the error system can be asymptotically stabilized by the presented method. Meanwhile, the sliding mode of the presented method starts at $t = 0$ and can be reached in the finite time, indicating that the errors are convergent to zero in the finite time as proven by Theorem 1. Although the curves of the control input almost make no difference, the presented method has better control performance in Figure 5.

Figure 6 depicts the phase plane trajectories of the error system (7), the nominal system (3) and the uncertain system (2).

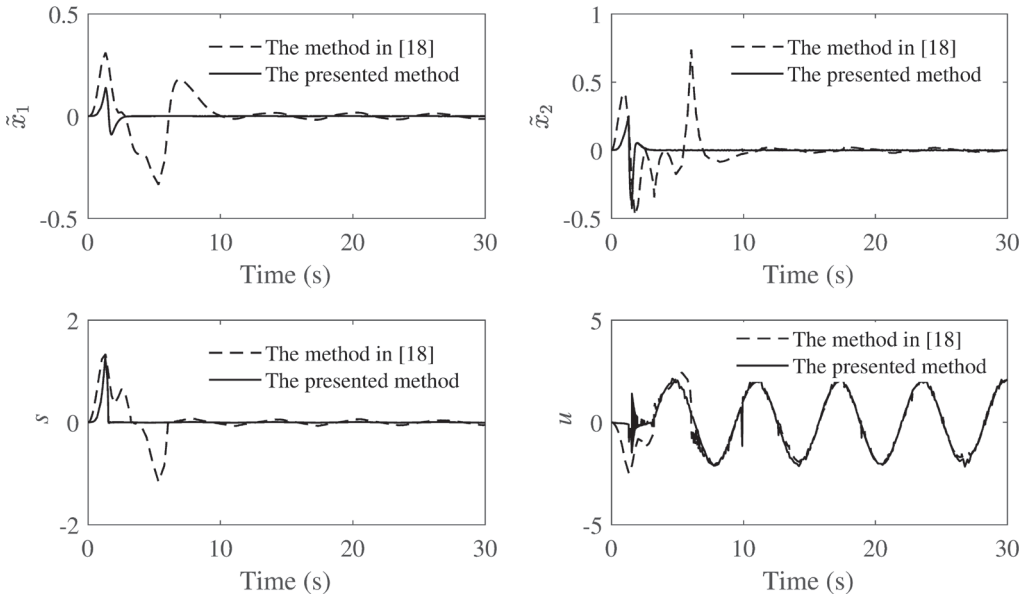

Fig. 5. Errors, sliding mode variable and control input in (7) in comparison with the benchmark under the effects of matched uncertainties

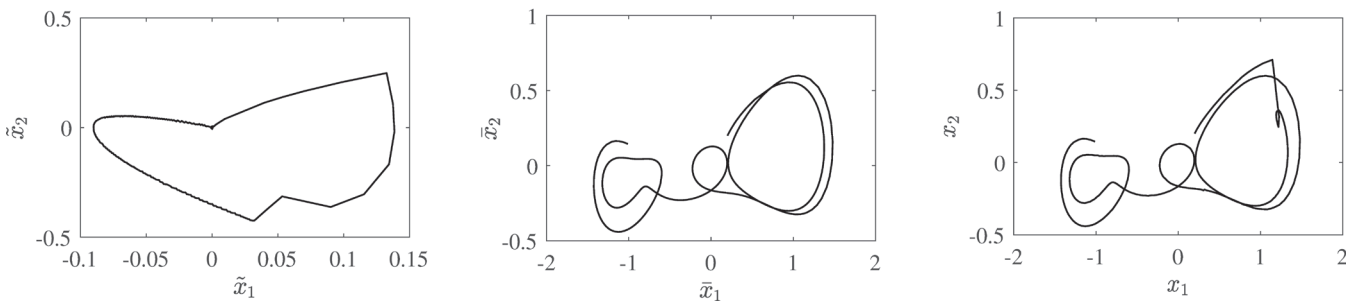

Fig. 6. Phase plane trajectories of the error system (7), the nominal system (3) and the uncertain system (2) under the effects of matched uncertainties

As proven by Theorem 2, the coronary artery system with matched uncertainties can synchronize the nominal coronary artery system by the presented method in Fig. 7. Meanwhile, the tracking errors can be convergent to zero in the limited time given in (14).

5.2. Mismatched uncertainties. Since the mismatched uncertainties can not be suppressed by the invariance of SMC, it is indispensable to illustrate their effects on the control performance. In order to illustrate the effects of mismatched uncertainties, d_1 is set to 0 and d_2 is set to be $2\sin(t)$. Under the condition, the other controller parameters are determined by $d^* = 2$, $d_0^* = 4.15$ and $\kappa = 6.0$. Figure 7 shows that the presented method can also suppress the chaotic phenomenon even if the mismatched uncertainties exist in the coronary artery system. Although the invariance of SMC can not overcome the mismatched uncertainties, the presented method can deal with them via the derivative-integral terminal sliding mode control design. Further, the sliding surface variable is also demonstrated. Compared with the curve by the method in [24], the sliding mode of the presented method can be reached at a shorter time and keep on sliding on the surface even if the mismatched uncertainties have adverse effects.

Figure 8 shows the phase plane trajectories of the error system (7), the nominal system (3) and the uncertain system (2) under the effects of mismatched uncertainties. Shown in Fig. 8, the coronary artery system with mismatched uncertainties can achieve the synchronization with the nominal coronary artery system as proven by Theorem 2.

Regardless of the kinds of uncertainties, the presented method in Figs. 5–8 can solve the adverse effects of the uncertainties and synchronize the uncertain coronary artery system with the nominal one. In clinic, the solution can contribute to the reduction and elimination of chaotic vasospasms, where the mechanism is to synchronize any chaotic blood vessels with a nominal one. The presented method can also benefit the research and development of clinical pharmacy for therapeutic purposes because medications can be treated as a kind of control input to suppress the chaotic vasospasms.

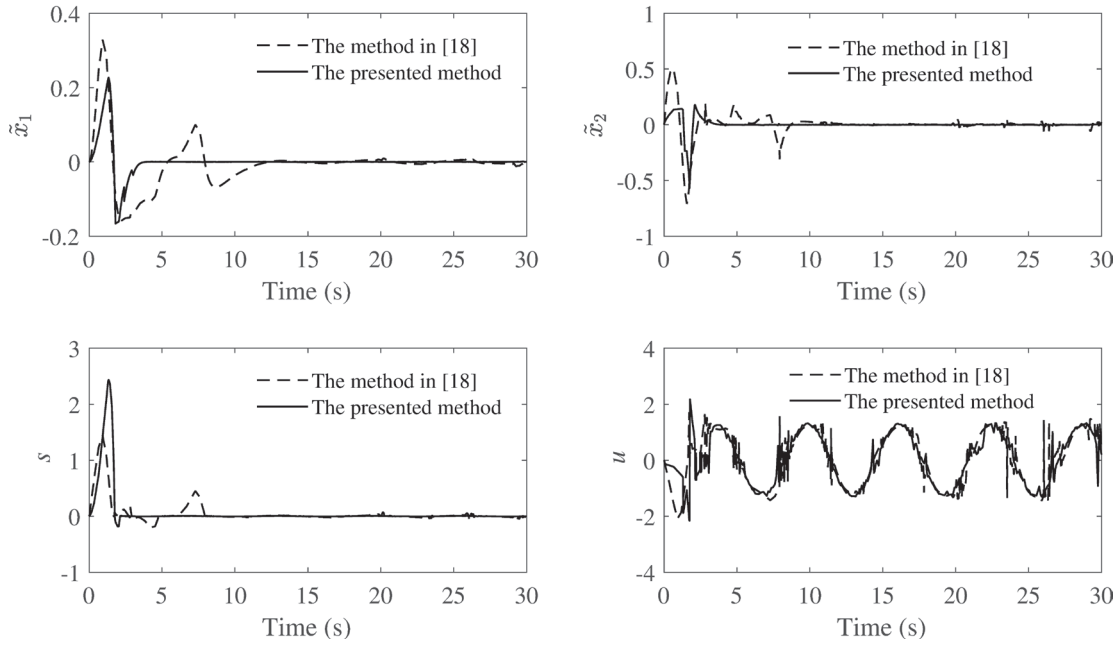

Fig. 7. Errors, sliding mode variable and control input in (7) in comparison with the benchmark under the effects of mismatched uncertainties

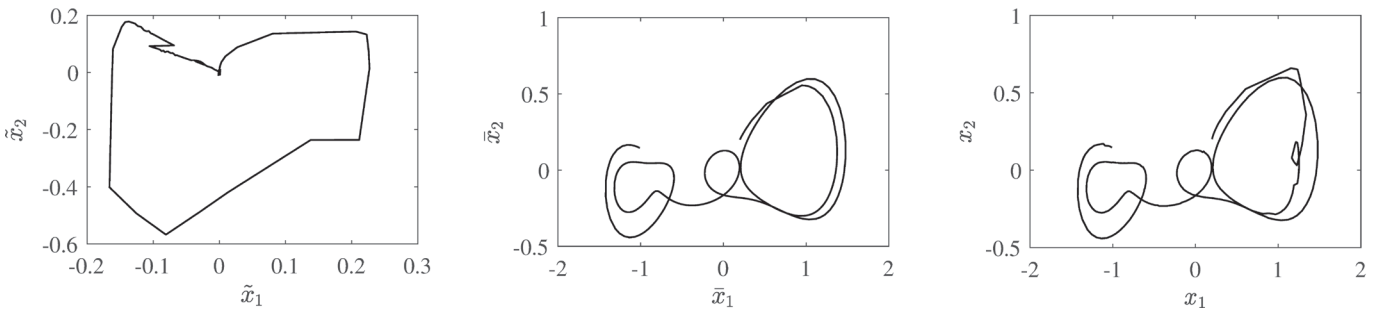

Fig. 8. Phase plane trajectories of the error system (7), the nominal system (3) and the uncertain system (2) under the effects of mismatched uncertainties.

6. Conclusions

Coronary artery disease can be induced by blood vessel spasms. Since the vasospasms can be considered as chaos in the aspect of engineering, this paper has explored the chaos synchronization problem of coronary artery systems. In order to have some insight into the bio-mathematical model of coronary artery systems, their nonlinear behaviors are presented by a series of bifurcation diagrams with respect to the changes of lumped parameters. The degree of complexity is described by the phase plane trajectory of coronary artery systems. The purpose is to synchronize any chaotic coronary arteries with a nominal one. Motivated by the purpose, the method of derivative-integral terminal sliding mode control is taken into consideration. Coronary artery systems suffer from uncertainties. Provided that the uncertainties have a known boundary, the stability of the presented approach has been proven in the sense of Lyapunov. The uncertainties integrate both matched and mismatched uncertainties, where the mismatched uncertainties can not be suppressed by the invariance. The simulation results via some comparisons have demonstrated the effectiveness, feasibility and robustness of the presented method regardless of uncertainties. The presented approach is beneficial to the research and development of clinical pharmacy.

Acknowledgements. This work was supported by the NSFC Project under Grant No.60904008, the Fundamental Research Funds for the Central Universities under Grant No.2018MS025 at North China Electric Power University and the Open Program from the State Key Laboratory of Management and Control for Complex Systems under Grant No. 20190113.

References

[1] G.K. Hansson, "Mechanisms of disease – Inflammation, atherosclerosis, and coronary artery disease", *N. Engl. J. Med*. 352 (16), 1685–1695 (2005).

[2] K. Ozaki and T. Tanaka, "Molecular genetics of coronary artery disease", *J. Hum. Genet*. 61 (1), 71–77 (2016).

[3] G.W. He and D.P. Taggart, "Spasm in arterial grafts in coronary artery bypass grafting surgery", *Ann. Thorac. Surg*. 101 (3), 1222–1229 (2016).

[4] T. Schauer, N.O. Negard, F. Previdi, H.J. Hunt, M.H. Fraser, E. Ferchland, and J. Raisch, "Online identification and nonlinear control of the electrically stimulated quadriceps muscle", *Control Eng. Practice* 13 (9), 1207–1219 (2005).

[5] W.L. Li, "Tracking control of chaotic coronary artery system", *Int. J. Syst. Sci*. 43 (1), 21–30 (2012).

[6] L.M. Pecora and T.L. Carroll, "Synchronization in chaotic systems", *Phys. Rev. Lett*. 64 (8), 821–824 (1990).

[7] M. Rafikov and J.M. Balthazar, "On control and synchronization in chaotic and hyperchaotic systems via linear feedback control", *Commun. Nonlinear Sci. Numer. Simul*. 13, 1246–1255 (2008).

[8] Y.G. Yu, H.X. Li, and J. Duan, "Chaos synchronization of a unified chaotic system via partial linearization", *Chaos Solitons Fractals* 41 (1), 457–463 (2009).

[9] D. Ghosh and A.R. Chowdhury, "Nonlinear observer-based impulsive synchronization in chaotic systems with multiple attractors", *Nonlinear Dyn*. 60 (4), 607–613 (2010).

[10] A. Chithra and I.R. Mohamed, "Synchronization and chaotic communication in nonlinear circuits with nonlinear coupling", *J. Comput. Electron*. 16 (3), 833–844 (2017).

[11] W.S. Wu, Z.S. Zhao, J. Zhang, and L.K. Sun, "State feedback synchronization control of coronary artery chaos system with interval time-varying delay", *Nonlinear Dyn*. 87 (3), 1773–1783 (2017).

[12] C. Gong, Y. Li, and X. Sun, "Backstepping control of synchronization for biomathematical model of muscular blood vessel", *J. Applied Sci*. 24 (6), 604–607 (2006).

[13] V.I. Utkin, *Sliding modes in control and optimization*, 2nd edn., Springer-Verlag, Berlin, 1992.

[14] D.W. Qian, S.W. Tong, H. Liu, and X.J. Liu, "Load frequency control by neural-network-based integral sliding mode for nonlinear power systems with wind turbines", *Neurocomputing* 173, 875–885 (2016).

[15] D.W. Qian, S.W. Tong, and C.D. Li, "Observer-based leaderfollowing formation control of uncertain multiple agents by integral sliding mode", *Bull. Pol. Ac.: Tech.* 65 (1), 35–44 (2017).

[16] D.W. Qian, C.D. Li, S.G. Lee, and C. Ma, "Robust Formation Maneuvers through Sliding Mode for Multi-agent Systems with Uncertainties", *IEEE/CAA Journal of Automatica Sinica* 5 (1), 342–351 (2018).

[17] J. Yang, M. Dou, and D. Zhao, "Iterative sliding mode observer for sensorless control of five-phase permanent magnet synchronous motor", *Bull. Pol. Ac.: Tech*. 65 (6), 845– 857 (2017).

[18] Y. Wang, M. Sun, S. Du, and Z. Chen, "Comparative investigations of nonlinear and linear observers for a highly manoeuvrable target in sliding mode guidance", *Bull. Pol. Ac.: Tech*. 65 (2), 233–245 (2017).

[19] C.J. Lin, S.K. Yang, and H.T. Yau, "Chaos suppression control of a coronary artery system with uncertainties by using variable structure control", *Comput. Math. Appl*. 64 (5), 988–995 (2012).

[20] Z.S. Zhao, X.M. Li, J. Zhang, and Y.Z. Pei, "Terminal sliding mode control with self-tuning for coronary artery system synchronization", *Int. J. Biomath*. 10 (3) (2017), DOI: 10.1142/S1793524517500413.

[21] A.M. Zou, K.D. Kumar, Z.G. Hou, and X. Liu, "Finite-Time attitude tracking control for spacecraft using terminal sliding mode and Chebyshev neural network", *IEEE Trans. Syst. Man Cybern. Part B-Cybern*. 41 (4), 950–963 (2011).

[22] C.D. Li, Z.X. Ding, J.Q. Yi, Y.S. Lv, and G.Q. Zhang, "Deep belief network based hybrid model for building energy consumption prediction", *Energies* 11 (1), 2018, DOI: 10.3390/en11010242.

[23] C.S. Chiu and C.T. Shen, "Finite-time control of DC-DC buck converters via integral terminal sliding modes", *Int. J. Electron*. 99 (5), 643–655 (2012).

[24] Z.S. Zhao, J. Zhang, G. Ding, and D.K. Zhang, "Chaos synchronization of coronary artery system based on higher order sliding mode adaptive control", *Acta Phys. Sin*. 64 (21), (2015), DOI: 10.7498/aps.64.210508.

[25] C.S. Chiu, "Derivative and integral terminal sliding mode control for a class of MIMO nonlinear systems", *Automatica* 48 (2), 316– 326 (2012).

[26] C.D. Li, Z.X. Ding, D.W. Qian, and Y.S. Lv, "Data-driven design of the extended fuzzy neural network having linguistic outputs", *J. Intell. Fuzzy Syst*. 34 (1), 349–360 (2018).

[27] C.D. Li, J.L. Gao, J.Q. Yi, and G. Zhang, "Analysis and design of functionally weighted single-input-rule-modules connected fuzzy inference systems", *IEEE Trans. Fuzzy Syst*. 26 (1), 56–71 (2018).

[28] C.D. Li, Z. Ding, D.B. Zhao, J.Q. Yi, and G.Q. Zhang, "Building energy consumption prediction: an extreme deep learning approach", *Energies* 10 (10), 1–20 (2017).